Nonlinear Integral Equations for Shape Reconstruction in the Inverse Interior Scattering Problem‡

Hai-Hua Qin[1] **and Fioralba Cakoni**[2]

[1] School of Mathematics and Statistics, Lanzhou University, Lanzhou, Gansu 730000, P. R. China

[2] Department of Mathematical Sciences, University of Delaware, Newark, Delaware 19716, USA

E-mail: cakoni@math.udel.edu and qinhh526@gmail.com

Abstract. In this paper, we consider the inverse scattering problem of recovering the shape of a perfectly conducting cavity from one source and several measurements placed on a curve inside the cavity. Under restrictive assumptions on the size of the cavity, a uniqueness theorem for finitely many excitations is given. Based on a system of nonlinear and ill-posed integral equations for the unknown boundary, we apply a regularized Newton iterative approach to find the boundary. We present the mathematical foundation of the method and give several numerical examples to show the viability of the method.

1. Introduction

Inverse obstacle scattering problems are typically viewed as exterior boundary value problems, see [2, 6], and such problems arise in many areas of applications including radar and sonar, medical imaging, geophysical exploration, and non-destructive testing. However, in some industrial applications of non-destructive testing it is important to test the structural integrity of cavities using acoustic or electromagnetic waves emitted and measured by sources and receivers respectively, placed inside the cavity [14]. In this case, the forward model of the scattering problem becomes an interior boundary value problem for the scattered field. The interior scattering problem was considered in [20,21] for the Dirichlet and impedance cavities respectively, where the authors applied the linear sampling method to recover the shape of the cavity from a knowledge of measured scattered fields on a curve inside the cavity due to sources placed on the same curve (see [2, 5, 7] for a discussion on the linear sampling method and other qualitative approaches). The advantage of the linear sampling method applied to this problem is

‡ The research of F.C. was supported in part by the U.S. Air Force Office of Scientific Research under Grant FA 9550-08-1-0138. The research of H.-H. Q was supported in part by a scholarship from the Postgraduate Scholarship Program of the China Scholarship Council and the NSF of China (10971089).

that it does not require any a priori knowledge of the size and physical properties of the cavity. Unfortunately, this method essentially needs a lot of data corresponding to multiple sources and receivers and the reconstruction is typically blurred. However, in some practical applications of non-destructive testing, it is important to resolve fine details of the surface of the cavity. Motivated by such a situation, in this paper we consider Newton type regularized iterative methods to reconstruct the boundary. These methods can be implemented with measurements corresponding to one probing source, provided that the type of the boundary condition on the surface of the cavity is known a priori and a good initial guess is available. If multiple probing is plausible, it is natural to apply a combination of a qualitative approach and optimization scheme; more precisely one could for instance first use the linear sampling method to obtain an initial guess and then initiate a Newton method to resolve more details. We remark that, as noted in [20], the interior scattering problem is physically more complicated in some way than the usual exterior scattering problem, since now all of the scattered waves are "trapped", i.e. the waves are repeatedly reflected off the boundary of the domain D. Also, the existence of eigenfrequencies associated with the cavity complicates the matter from physical and mathematical point of view.

To fix our ideas, we consider the scattering of an electromagnetic time harmonic point source located inside a perfectly conducting infinite cylinder with cross section a bounded simply connected domain $D \subset \mathbb{R}^2$ with a C^2 boundary ∂D. Assuming that the electric field is polarized in the TM mode this leads to an interior Dirichlet boundary value problem for the $\mathbb{R}^2$-Helmholtz equation inside D. The goal is to determine the boundary ∂D from a knowledge of the measured scattered field on a smooth curve C inside D due to a single point source situated on C. Based on a single-layer potential ansatz for the scattered field with density φ living on the boundary ∂D we transform our inverse problem into a system of nonlinear and ill-posed integral equations, and then use a regularized Newton type iterative approach to reconstruct the shape of the cavity. Nonlinear integral equation approach was suggested in [16] to determine the shape of a perfectly conducting inclusion within a homogeneous conducting medium modeled by the Laplace equation. Then, this idea has been further developed and applied to variety of inverse boundary value problems in scattering and electrostatics [3, 4, 10–13, 15, 17]. Our single layer potential approach follows the ideas in [3]. An alternative nonlinear integral equation method based on Green's representation formula similar to the approach in [16] could be developed for our interior inverse scattering problem, but this method is not subject of our study.

The plan of our paper is as follows. In the next section we formulate mathematically the inverse problem, then following the idea of [8], show that under size restriction the boundary of the cavity is uniquely determined from one measurement, and finally derive a system of nonlinear integral equations equivalent to our inverse problem. In Section 3 we describe the linearization process, show the injectivity of the linearized system and give two iteration schemes to reconstruct the boundary. We conclude our paper by providing several numerical examples to show the feasibility of the proposed methods.

2. Formulation of the problem

Let a simply connected domain $D \subset \mathbb{R}^2$ with C^2 boundary ∂D be the cross section of an infinite cylinder, and consider a TM polarized time harmonic electric dipole located inside this cylinder. Then the only component u^s of the scattered electric field inside the cylinder satisfies

$$\Delta u^s + k^2 u^s = 0 \quad \text{in} \quad D, \tag{1}$$

$$u^s = -\Phi(\cdot, d) \quad \text{on} \quad \partial D, \tag{2}$$

i.e. the total field $u = u^s + \Phi(\cdot, d)$ satisfies $u = 0$ on ∂D, where $k > 0$ is the wave number, $d \in D$ is a fixed point, and $\Phi(\cdot, d)$ is the fundamental solution of the Helmholtz equation defined by

$$\Phi(x, d) = \frac{i}{4} H_0^{(1)}(k|x - d|)$$

with $H_0^{(1)}$ being a Hankel function of the first kind of order zero. It is well known (see e.g. [2]) that for $\Phi(\cdot, d) \in H^{\frac{1}{2}}(\partial D)$ there exists a unique solution $u^s \in H^1(D)$ for the direct problem (1)-(2) provided k^2 is not a Dirichlet eigenvalue for $-\Delta$ in D. From now on we assume that k^2 is not a Dirichlet eigenvalue for $-\Delta$ in D. We remark that for the Dirichlet interior scattering problem the presence of eigenfrequencies is detrimental to the problem as oppose to the exterior scattering problem. Physically, if the cavity is a perfect reflector, probing with a source at an eigenfrequency resolves to a resonance state. An impedance type boundary condition could be a good physical model for the cavity since in practice waves always penetrate a little bit through the boundary. Such a model does not suffer from the existence of eigenfrequencies.

Now let $C \subset D$ be a closed smooth curve inside D, and assume that for a fixed $d \in C$ we know

$$u^s|_C := u^s(x, d), \qquad \text{for all } x \in C. \tag{3}$$

The *inverse problem* we are concerned with in this paper is to determine ∂D from the measured data u^s on the curve C. A general uniqueness theorem is provided in [20] where it is proven that a knowledge of $u^s(\cdot, d)|_C$ for all $d \in C$ (or if C is analytic for $d \in C_0 \subset C$) uniquely determines ∂D (under more general assumption of ∂D being Lipshitz). A general uniqueness theorem with one (or finitely many) measurements for the interior scattering problem is still an open problem. However, in the following theorem we are able to adapt the idea of Colton and Sleeman [8] (see also [6]) to show that the boundary of a small cavity can be uniquely determined from finitely many measurements. To this end for the purpose of the theorem and in the following, we assume that k^2 is not a Dirichlet eigenvalue for the negative Laplacian in the interior of C (this is not a restriction since we can modify the measurement curve C see Remark 2.4). Also, due to the nature of the problem we assume a priori that D contains the domain, hereafter denoted by $\dot{C}$, circumscribed by the measurements curve C.

Theorem 2.1. *Assume that D_1 and D_2 are two bounded simply connected regions containing C and contained in a disk of radius R, and let*

$$N := \sum_{t_{0l}<kR} 1 + \sum_{t_{nl}<kR, n\neq 0} 2, \tag{4}$$

where $t_{nl}(l = 0, 1, \cdots; n = 0, 1, \cdots)$ denote the positive zeros of the Bessel functions J_n, i.e. $J_n(t_{nl}) = 0$. Denote by $u_1^s(\cdot, d)$ and $u_2^s(\cdot, d)$ the scattered field corresponding to D_1 and D_2 respectively, due to the point source $\Phi(\cdot, d)$. If $u_1^s(\cdot, d)$ and $u_2^s(\cdot, d)$ coincide on C for $N + 1$ distinct locations $d \in C$ and one fixed wave number k, then $D_1 = D_2$.

Proof. Assume by contradiction that $D_1 \neq D_2$ are two bounded domains and u_i^s, $i = 1, 2$, satisfy (1)-(2) with D replaced by D_i, respectively. Proceeding as in the proof of Theorem 2.1 in [20], if for a fixed $d \in C$, $u_1^s(x, d) = u_2^s(x, d)$ for all $x \in C$ and letting $v = u_1^s - u_2^s$, we have that

$$\begin{aligned} &\Delta v + k^2 v = 0 \quad \text{in} \quad \dot{C}, \\ &v = 0 \quad \text{on} \quad C. \end{aligned}$$

Since k^2 is not a Dirichlet eigenvalue for the interior of C, we can conclude that $v = 0$ in $\dot{C} \bigcup C$. Let $D_0 = D_1 \bigcap D_2$, which by the nature of the problem is assumed to contain $\dot{C}$. In the case when D_0 has multiple components we consider the component containing $\dot{C}$ (still denoted by D_0); such a component always exists due to the assumption that both D_1 and D_2 contain $\dot{C}$. The by the unique continuation principle, we have that $v = 0$ in D_0 and an application of the trace theorem yields $v = 0$ on ∂D_0, i.e. $u_1^s(\cdot, d) = u_2^s(\cdot, d)$ on ∂D_0. Without loss of generality, we assume that $D_2 \setminus (\overline{D_1} \bigcap \overline{D_2})$ is nonempty and denote by D^* one of the simply connected components of $D_2 \setminus (\overline{D_1} \bigcap \overline{D_2})$. Then, $u_2^s(\cdot, d)$ satisfies

$$\begin{aligned} &\Delta u_2^s + k^2 u_2^s = 0 \quad \text{in} \quad D^*, \\ &u_2^s(\cdot, d) = -\Phi(\cdot, d) \quad \text{on} \quad \partial D^* \end{aligned}$$

due to the fact that $u_2^s(\cdot, d)$ equals to $u_1^s(\cdot, d)$ on ∂D_0 and the boundary condition for $u_2^s(\cdot, d)$ on ∂D_2. Now let $w(\cdot, d) = u_2^s(\cdot, d) + \Phi(\cdot, d)$, for fixed $d \in C$. Since d is not in $\overline{D^*}$ then

$$\Delta w + k^2 w = 0 \quad \text{in} \quad D^*, \tag{5}$$

$$w(\cdot, d) = 0 \quad \text{on} \quad \partial D^*. \tag{6}$$

Hence, $w \in H_0^1(D^*)$ is a Dirichlet eigenfunction for the negative Laplacian in the domain D^* corresponding to the eigenvalue k^2. Next we show that the eigenfunctions $w(\cdot, d_n)$, $d_n \in C, n = 1, \cdots, N + 1$ corresponding to the same eigenvalue k^2 are linearly independent provided that D_1 and D_2 are included in a ball of radius R and N is defined by (4). To this end consider

$$\sum_{n=1}^{N+1} c_n w(\cdot, d_n) = 0 \tag{7}$$

in D^*. By the unique continuation principle, the equation (7) holds also in a neighborhood of C exterior to $\dot{C}$. Now for a fixed $m \in [1, N+1]$, choose $h > 0$ sufficiently small, such that $x_s^m = d_m + \frac{h}{s}\nu(d_m)$, $s = 1, 2, \cdots$, is in a neighborhood of d_m. Then we have

$$c_m \Phi(x_s^m, d_m) = - \sum_{n=1, n\neq m}^{N+1} c_n \Phi(x_s^m, d_n).$$

Note that $\Phi(x_s^m, d_m)$ becomes unbounded whereas $\sum_{n=1,n\neq m}^{N+1} c_n \Phi(x_s^m, d_n)$ remains bounded as s tends to infinity. Hence, $c_m = 0$ for $1 \leq m \leq N+1$, i.e. $w(\cdot, d_n)$, $n = 1, \cdots, N+1$, are linearly independent.

We now proceed exactly in the same way as in the proof of Theorem 5.2 in [6]. Let B_R be a disk of radius R containing both D_1 and D_2 and let $0 < \lambda_1 \leq \lambda_2 \leq \cdots \leq \lambda_m = k^2$ be the Dirichlet eigenvalues of D^* less than or equal to k^2. Based on the the strong monotonicity property for the Dirichlet eigenvalues of the negative Laplacian we can obtain that the multiplicity M of λ_m is less than or equal to the sum of the multiplicities N of the eigenvalues for the disk B_R which are less than k^2, i.e. $M \leq N$, which contradicts the fact that $N+1$ distinct directions yield $N+1$ linearly independent eigenfunctions with eigenvalue k^2 for D^*. Hence, $D_1 = D_2$. □

The following corollary is a straight forward consequence of the previous theorem.

Corollary 2.2. *Assume that D_1 and D_2 are two bounded simply connected regions containing C and contained in a disk of radius R such that $kR < t_0$, where $t_0 (\approx 2.40483)$ is the smallest positive zero of the Bessel function J_0. If the measured data $u^s(\cdot, d)$ on C coincide for one location $d \in C$ and one fixed wave number k, then $D_1 = D_2$.*

Remark 2.3. Following the idea of [9] for a given R it is possible to reduce by half the number of probing sources in Theorem 2.1 and replace t_0 in Corollary 2.2 by the first positive zero of J_1, i.e. $t_{10} \approx 3.83171$. In general the uniqueness with finitely many incident waves is an open question.

Remark 2.4. The assumption that k^2 is not a Dirichlet eigenvalue for the negative Laplacian in the interior of C is not a restriction since we have the freedom to choose such a measurement curve C. In particular by virtue of the Faber-Krahn inequality for the first Dirichlet eigenvalue of $\dot{C}$ (the latter is greater than $\pi k_{01}^2/|\dot{C}|$ where k_{01}^2 is the first zero of the Bessel function J_0) it is always possible to reduce the size of C so that the given k^2 is not an eigenvalue. Also note that Theorem 2.1 and everything in the following hold valid if C is replaced by an open arc $C_0 \subset C$ if C ia an analytic curve for which k^2 is not a Dirichlet eigenvalue.

Now we turn our attention to the reconstruction of ∂D from a knowledge of the measured scattered field $u^s(\cdot, d)|_C$ for one single point source located at $d \in C$. We start by representing the scattered field as a single layer potential

$$u^s(x) = (\mathcal{S}\varphi)(x) := \int_{\partial D} \Phi(x, y)\varphi(y) ds(y), \qquad x \in D \tag{8}$$

with a unknown density $\varphi \in L^2(\partial D)$ over the unknown boundary ∂D, and introducing the boundary integral operators

$$S_j : L^2(\partial D) \mapsto L^2(\Gamma_j),\ j = 0, 1$$

defined by

$$(S_j\varphi)(x) := \int_{\partial D} \Phi(x, y)\varphi(y)ds(y),\ x \in \Gamma_j, \tag{9}$$

where $\Gamma_0 = \partial D$ and $\Gamma_1 = C$. Note that the ansatz (8) is always possible since due to the assumption that k^2 is not a Dirichlet eigenvalue for the negative Laplacian in D, we have that $\mathcal{S} : L^2(\partial D) \to H^{3/2}_{loc}(\mathbb{R}^2 \setminus \partial D)$, is invertible (see e.g. [18]). Letting x in (8) approach ∂D (from inside) and using (2) we obtain

$$S_0\varphi = -\left.\Phi(\cdot, d)\right|_{\partial D}. \tag{10}$$

From (3) we also have

$$S_1\varphi = \left.u^s(\cdot, d)\right|_C. \tag{11}$$

Hence, we have that the boundary ∂D and the density $\varphi \in L^2(\partial D)$ in the representation (8) of the corresponding scattered field $u^s(\cdot, d)$, satisfy the system of (nonlinear) integral equations (10) and (11). Conversely, if the closed curve ∂D and the density φ satisfy the system (10)-(11) then ∂D is the solution of the inverse problem. Indeed, if we define u^s by (8) then from (10) and (11) we have that u^s satisfies equations (1)-(3). Hence we can state the following theorem.

Theorem 2.5. *The inverse problem and the system of integral equations (10) and (11) are equivalent.*

We note that for a given ∂D the operator $S_1 : L^2(\partial D) \to L^2(C)$ is a compact integral operator with analytic kernel, thus (11) is severely ill-posed. To solve the system of nonlinear integral equations (10) and (11) we propose two possible techniques. The first technique (referred to as Method A in Section 3) is to solve simultaneously both equations using a regularized iterative Newton linearization method. Alternatively, we can use an alternating scheme (referred to as Method B in Section 3), for which, given ∂D, we solve the ill-posed equation (11) for φ then plug the solution in (10) and solve the linearized version of (10) to find an update for ∂D and then iterate (the latter could be seen as a way to separate nonlinearity from the ill-posedness). The following lemma is needed to apply the Tikhonov regularization technique to the severely ill-posed integral equation (11) in particular in the implementation of Method B.

We recall that we have assumed that k^2 is not a Dirichlet eigenvalue for $-\Delta$ in D as well in the region bounded by C.

Theorem 2.6. *The operator $S_1 : L^2(\partial D) \to L^2(C)$ is injective and has dense range.*

Proof. Let $S_1\varphi = 0$ on C. Define

$$v(x) = \int_{\partial D} \Phi(x, y)\varphi(y)ds(y), \qquad x \in \mathbb{R}^2 \backslash \partial D.$$

Note that v satisfies $\triangle v+k^2 v=0$ inside the region bounded by the curve C and $v|_C=0$. Since k^2 is not an interior Dirichlet eigenvalue we obtain that $v=0$ in the interior of C (cf. [1]). The unique continuation principle leads to $v=0$ in D and then $v|_{\partial D}=0$ from inside D. Furthermore, we also have that v satisfies $\triangle v+k^2 v=0$ in $\mathbb{R}^2\backslash\bar{D}$ together with the Sommerfeld radiation condition

$$\lim_{r\to\infty}\sqrt{r}\left(\frac{\partial v}{\partial r}-ikv\right)=0,$$

where $r=|x|$. By continuity of the single layer potential across ∂D we in addition have that $v|_{\partial D}=0$ from outside of D. By uniqueness of the exterior Dirichlet boundary value problem for the Helmholtz equation we conclude that $v=0$ in $\mathbb{R}^2\backslash\bar{D}$. Hence, an application of the jump relation for the gradient of the single layer potential yields $\varphi=0$ on ∂D, i. e. the operator S_1 is injective. Next, we show that S_1 has dense range. Straightforward calculation show that the L^2- adjoint $S_1^*: L^2(C)\to L^2(\partial D)$ of the operator S_1 is given by

$$(S_1^*\phi)(x)=\overline{\int_C \Phi(x,y)\overline{\phi(y)}ds(y)},\qquad x\in\partial D.$$

Since $N(S_1^*)^\perp=\overline{S_1(L^2(\partial D))}$, to complete the proof of the theorem we need to show that S_1^* is injective. To this end let now $S_1^*\phi=0$ on ∂D and define

$$w(x)=\int_C \Phi(x,y)\overline{\phi(y)}ds(y),\ x\in\mathbb{R}^2\backslash C.$$

Then $w=0$ on ∂D. By the similar argument employed to show the injectivity of S_1 (first using the uniqueness of the exterior problem for D, then after an analyticity argument using the uniqueness for interior problem inside C) we can obtain that $\phi=0$ on C, concluding that S_1^* is injective whence S_1 has dense range. □

3. Iterative solution of the inverse problem

The main goal in this section is to develop iterative solution schemes to solve the system of nonlinear integral equations (10) and (11) for the unknown boundary ∂D. Due to nonlinearity with respect to ∂D we need to linearize the system which requires computing the Fréchet derivative of integral operators with respect to the boundary. To this end we first need to parametrize the boundary and the involved integral operators.

3.1. Parameterization of the integral equations

We start by a parameterization of the boundary ∂D and the measurements curve C which are assumed to be C^2-smooth curves, namely

$$\partial D:=\{z(t)=(z_1(t),z_2(t)):t\in[0,2\pi]\} \tag{12}$$

and

$$C:=\{\rho(t)=(\rho_1(t),\rho_2(t)):t\in[0,2\pi]\}$$

where the 2π periodic C^2-smooth functions $z, \rho : \mathbb{R} \mapsto \mathbb{R}^2$ are injective on $[0, 2\pi]$ satisfying $z'(t) \neq 0$ and $\rho'(t) \neq 0$ for all t. We set

$$\psi(t) := |z'(t)|\varphi(z(t))$$

and for any vector $a = (a_1, a_2)$ we denote by $a^\perp = (a_2, -a_1)$, that is $a^\perp$ is obtained by rotating a clockwise by 90 degrees. We obtain the parameterized form of the integral operators (9), denoted now by A_j $(j = 0, 1)$ and given by

$$[A_0(z, \psi)](t) = \frac{i}{4} \int_0^{2\pi} H_0^{(1)}(k|z(t) - z(\tau)|)\psi(\tau)d\tau \tag{13}$$

$$[A_1(z, \psi)](t) = \frac{i}{4} \int_0^{2\pi} H_0^{(1)}(k|\rho(t) - z(\tau)|)\psi(\tau)d\tau \tag{14}$$

for $t \in [0, 2\pi]$, where $\psi \in L^2[0, 2\pi]$ and $z \in C^2[0, 2\pi]$. For simplicity we set $\omega_0(z) := -\Phi(z, d)$ which assumes the form

$$[\omega_0(z)](t) = -\frac{i}{4} H_0^{(1)}(k|z(t) - d|), \qquad t \in [0, 2\pi]. \tag{15}$$

and write the measured data $\omega_1(\rho(t)) := u^s(\rho(t), d)$ as a function of $t \in [0, 2\pi]$. Then the system (10)-(11) is transformed to

$$A_0(z, \psi) = \omega_0(z), \tag{16}$$

$$A_1(z, \psi) = \omega_1. \tag{17}$$

The kernel of the operator A_1 is of course analytic whereas in order to analyze the kernel of the operator A_0 which is

$$M(t, \tau) = \frac{i}{4} H_0^{(1)}(k|z(t) - z(\tau)|)$$

for $t \neq \tau$, we split it into [6]

$$M(t, \tau) = M_1(t, \tau) \ln\left(4 \sin^2 \frac{t - \tau}{2}\right) + M_2(t, \tau),$$

where

$$M_1(t, \tau) := -\frac{1}{4\pi} J_0(k|z(t) - z(\tau)|)$$

and the diagonal term for M_2 is given by

$$M_2(t, t) = \frac{i}{4} - \frac{E}{2\pi} - \frac{1}{4\pi} \ln\left(\frac{k^2}{4}|z'(t)|^2\right),$$

where E denotes the Euler's constant.

3.2. Two iteration schemes

We now turn to the iteration schemes for solving (16)-(17). In this paper, we consider two ways to solve the system (16) - (17), which are also discussed in [11] for the exterior scattering problem.

Method A. This method involves the full linearization of the system (16) - (17) with respect to ψ and z which leads to

$$A_0(z,\psi) + A_0(z,\chi) + A_0^{'}[z,\psi]\zeta = \omega_0(z) + \omega_0^{'}(z)\zeta, \tag{18}$$

$$A_1(z,\psi) + A_1(z,\chi) + A_1^{'}[z,\psi]\zeta = \omega_1. \tag{19}$$

The operators $A_0^{'}[z,\psi]\zeta$, $A_1^{'}[z,\psi]\zeta$ and $\omega_0^{'}(z)\zeta$ denote the Fréchet derivatives with respect to z in the direction ζ of the operators $A_0(z,\psi)$, $A_1(z,\psi)$ and $\omega_0(z)$, respectively. Solving the inverse problem for ∂D via (18) and (19) can be summarized by the following algorithm:

(i) We make an initial guess for the boundary ∂D, i.e. for $z(t)$, $t \in [0,\, 2\pi]$ and solve the severely ill-posed equation (17) to get the corresponding initial guess for ψ.

(ii) Having now an approximation for z and ψ, the linear system (18) - (19) is solved for ζ and χ to obtain the update $z+\zeta$ and $\psi+\chi$.

(iii) The second step is repeated until a suitable stopping criterion is satisfied.

Method B. This method is to decompose the inverse problem into a severely ill-posed linear problem and a mildly ill-posed nonlinear problem (cf. [3]). Here only the equation (16) is linearized with respect to z, and the procedure alternates between

$$A_1(z,\psi) = \omega_1 \tag{20}$$

and

$$A_0(z,\psi) + A_0^{'}[z,\psi]\zeta = \omega_0(z) + \omega_0^{'}(z)\zeta. \tag{21}$$

The algorithm can be summarized as follows:

(i) We start with an initial guess for the boundary ∂D, i.e. for $z(t)$, $t \in [0,\, 2\pi]$.

(ii) Solve the severely ill-posed linear equation (17) to get the density ψ.

(iii) Plug in (21), ψ found in step 2 and solve (21) for ζ to obtain the update $z+\zeta$ for the boundary.

(iv) The second and the third steps are repeated until a suitable stopping criterion is satisfied.

We remark that there is also a third possibility for iterative solution of (16) and (17) which we do not investigate in this paper. Reversing the roles of the equations in Method B, one can first solve the well-posed equation (16) for the the density and then linearize the ill-posed equation (17) to update the boundary. This method corresponds to the version proposed in [15] for the exterior scattering problem. Note that Method B resembles the hybrid method that has investigated by Kress and Serranho in a number of papers (see e.g. [10] and the references therein).

The Fréchet derivatives of the operators A_0, A_1 are computed by formally differentiating the kernels of integral operators with respect to z (see [19]) whereas ω_0' is obtained by direct differentiation with respect to z. Their explicit expressions are given by

$$A_0^{'}[z,\psi]\zeta(t) = -\frac{ik}{4}\int_0^{2\pi} H_1^{(1)}(k|z(t)-z(\tau)|)\frac{(z(t)-z(\tau))\cdot(\zeta(t)-\zeta(\tau))}{|z(t)-z(\tau)|}\psi(\tau)d\tau,$$

$$A_1^{'}[z,\psi]\zeta(t) = \frac{ik}{4}\int_0^{2\pi} H_1^{(1)}(k|\rho(t)-z(\tau)|)\frac{(\rho(t)-z(\tau))\cdot\zeta(\tau)}{|\rho(t)-z(\tau)|}\psi(\tau)d\tau,$$

$$\omega_0^{'}(z)\zeta(t) = \frac{ik}{4}H_1^{(1)}(k|z(t)-d|)\frac{(z(t)-d)\cdot\zeta(t)}{|z(t)-d|}$$

for $t \in [0, 2\pi]$. We note that the kernel for the operator $A_1^{'}$ is analytic whereas to understand the singularity of the kernel of the operator $A_0^{'}$ which is

$$L(t,\tau) = -\frac{ik}{4}H_1^{(1)}(k|z(t)-z(\tau)|)\frac{(z(t)-z(\tau))\cdot(\zeta(t)-\zeta(\tau))}{|z(t)-z(\tau)|}.$$

We split it into

$$L(t,\tau) = L_1(t,\tau)\ln\left(4\sin^2\frac{t-\tau}{2}\right) + L_2(t,\tau),$$

where

$$L_1(t,\tau) = \frac{k}{4\pi}J_1(k|z(t)-z(\tau)|)\frac{(z(t)-z(\tau))\cdot(\zeta(t)-\zeta(\tau))}{|z(t)-z(\tau)|}$$

and notice that the diagonal term $L_2(t,t)$ is given by

$$L_2(t,t) = -\frac{1}{2\pi}\frac{z'(t)\cdot\zeta'(t)}{|z'(t)|^2}.$$

Next we show the injectivity for the linearized system (18) - (19) at the exact solution. We remind the reader once more that the assumption that k^2 is not a Dirichlet eigenvalue for $-\Delta$ in D as well in the region bounded by C, is still in place. In the following, without loss of generality we can assume that the perturbation ζ is in the direction of the normal to the boundary.

Theorem 3.1. *Let z be the parameterization of the exact boundary ∂D and let $\psi = |z'|\varphi\circ z$ where φ satisfies equations (10)-(11). Assume that $\zeta = q[z']^{\perp} \in C^2[0,2\pi]$ for a scalar q and $\chi \in L^2[0,2\pi]$ satisfy the homogeneous system*

$$A_0(z,\chi) + A_0^{'}[z,\psi]\zeta = \omega_0^{'}(z)\zeta, \tag{22}$$

$$A_1(z,\chi) + A_1^{'}[z,\psi]\zeta = 0. \tag{23}$$

Then $\chi = 0$ and $\zeta = 0$.

Proof. Following [16] we define

$$W(x) := \int_0^{2\pi}\Phi(x,z(\tau))\chi(\tau)d\tau - \int_0^{2\pi}\nabla_x\Phi(x,z(\tau))\cdot\zeta(\tau)\psi(\tau)d\tau, \quad x\in\mathbb{R}^2\backslash\partial D. \tag{24}$$

From (23) we obtain that $W|_C = 0$ and since W satisfies $\Delta W + k^2 W = 0$ inside C and since k^2 is not an interior Dirichlet eigenvalue we have that $W = 0$ inside C (cf. [1]). The unique continuation principle leads to $W = 0$ in D and an application of the trace theorem leads to $W|_{\partial D} = 0$. Then by the jump relations for the single-layer and double-layer potentials, letting x tend to the boundary ∂D from inside D, we obtain

$$\int_0^{2\pi} \Phi(z(t), z(\tau))\chi(\tau)d\tau - \frac{1}{2}\zeta(t)\cdot\nu(z(t))\frac{\psi(t)}{|z'(t)|} - \int_0^{2\pi} \nabla_{z(t)}\Phi(z(t), z(\tau))\cdot\zeta(\tau)\psi(\tau)d\tau = 0, \tag{25}$$

where ν denotes the outward unit normal to ∂D. Combining (22) and (25), we have

$$\frac{1}{2}\zeta(t)\cdot\nu(z(t))\frac{\psi(t)}{|z'(t)|} + \zeta(t)\cdot\int_0^{2\pi} \nabla_{z(t)}\Phi(z(t), z(\tau))\psi(\tau)d\tau - \omega_0^{'}(z)\zeta = 0.$$

Thus

$$\zeta\cdot\nabla(u^s + \Phi(\cdot, d))\circ z = 0 \quad \text{on} \quad \partial D$$

which means that

$$\zeta\cdot\nu(z)\left(\frac{\partial(u^s + \Phi(\cdot, d))}{\partial\nu}\circ z\right) = 0 \quad \text{on} \quad \partial D.$$

On the other hand we also have $u^s + \Phi(\cdot, d) = 0$ on ∂D. Now if $\zeta\cdot\nu(z) \neq 0$ on an open interval $I \subset [0, 2\pi]$, then the Holmgren's theorem implies that $u^s + \Phi(\cdot, d) = 0$ in a neighborhood of C exterior to C. In particular,

$$u^s(x_n) = -\Phi(x_n, d)$$

where $x_n = d + \frac{h}{n}\nu(d)$, $n = 1, 2, \cdots$ are chosen in a neighborhood of $d \in C$ for sufficiently small $h > 0$. Letting now $n \to \infty$ we observe that u^s is bounded but Φ is unbounded, which leads to a contradiction. Hence $\zeta\cdot\nu(z) = 0$, i. e. $q[z']^\perp\cdot[z']^\perp = 0$ which means $\zeta = 0$. Now W becomes

$$W(x) = \int_0^{2\pi} \Phi(x, z(\tau))\chi(\tau)d\tau,\ x \in \mathbb{R}^2\backslash\partial D.$$

From (23) we have $W|_C = 0$. Since k^2 is not an interior Dirichlet eigenvalue $W = 0$ inside C and, by the unique continuation principle, also in D and hence $W|_{\partial D} = 0$. Since W satisfies the Sommerfeld radiation condition and by the uniqueness of the exterior Dirichlet boundary value problem for the Helmholtz equation, we have that $W = 0$ in $\mathbb{R}^2\backslash\overline{D}$. Finally, by the jump relation for the gradient of the single-layer potential we obtain that $\chi = 0$. □

Remark 3.2. Our approach is based on the use of single- and double- layer potentials with kernel the fundamental solution of the Helmholtz equation, which is a natural choice for the given homogeneous medium inside the cavity. The integral equation approach typically brings into the analysis both the interior and exterior problems.

Since our potentials satisfy the Sommerfeld radiation condition we use it. If a different representation is considered one has to use respective external conditions.

We end this section by remarking that the mathematical justification of the use of Tikhonov regularization for solving the severely ill-posed linear equation (17) for a fixed ∂D is provided by Theorem 2.6.

4. Numerical examples

In this section we present several numerical examples to show the effectiveness of both Method A and Method B. For the sake of simplicity, in the following numerical computations we assume that the interior curve C is a circle, i. e. $C = \{\rho(t)|\,\rho(t) = r_c(\cos t, \sin t), t \in [0, 2\pi]\}$ where $r_c > 0$ is a constant. The synthetic data u^s on the curve C is obtained by solving the direct problem (1)-(2) using a double-layer potential approach in which the involved integral equation is solved by Nyström's method [6]. For the solution of the inverse problem we use the iteration procedures described in Section 3.2 to obtain an approximation for the boundary ∂D. We apply the trapezoidal rule to discretize integral equations occurring in (18)-(19) and (20)-(21) with N equidistant grid points and use Tikhonov regularization technique to solve them with L^2 penalty term for the density ψ, and the updates χ and ζ. Recalling the form $\zeta = q[z']^\perp$ of the boundary perturbation, the magnitude q of the normal perturbation is approximated by a trigonometric polynomial of degree less than or equal to $m \in \mathbb{N}$, i.e.

$$q(t) \approx \sum_{j=0}^{m} a_j \cos(jt) + \sum_{j=1}^{m} b_j \sin(jt).$$

The corresponding regularization parameters are denoted as α_ψ, α_χ and α_ζ, which are chosen by trial and error. In the implementation of Method B, the regularization parameters α_ψ and α_ζ once chosen are kept constant in each iteration, whereas in the implementation of Method A we find out that it is best to change the regularization parameters at each step of iterations according to $\widetilde{\alpha_{\chi,j}} = (1/6)^j \alpha_\chi$ and $\widetilde{\alpha_\zeta} = (1/6)^j \alpha_\zeta$, $j = 1, \cdots, itera$, where the "itera" denotes the number of iterations. For Method B we need an additional regularization by updating the density ψ according to $\psi_{new} = \lambda\psi + (1-\lambda)\psi_{old}$ where ψ is the solution of equation (17) and λ is chosen between 0.4 and 0.6; the need for such correction is also observed in [3] and [16].

Of course, as mentioned in the description of Method A and Method B, a suitable stopping criterion is needed. In our numerical examples we chose the number of iterations by trial and error. We study the sensitivity of the relative ℓ^2 error of the reconstructions with respect to the number of the iterations, and the results are presented in Fig. 9.

In our computations, we always take the source point $d = r_c(-1, 0)$ and choose as the initial guess for the boundary a circle centered at the origin with radius r_o to start the iterations.

As a first example we consider a peanut parametrized by

$$\partial D_p = 0.8\sqrt{\cos^2 t + 0.25\sin^2 t}\,(\cos t, \sin t)\,, \quad 0 \le t \le 2\pi. \tag{26}$$

The numerical results are shown in Figs. 1 - 2 where the involved parameters are chosen according to $r_c = 0.1$, $r_o = 0.3$, $m = 11$, $N = 56$ and $k = 2$. For the reconstructions shown in Figs. 1(a) and 2(a) we use exact data and pick $\alpha_\psi = \alpha_\chi = 10^{-10}$ and $\alpha_\zeta = 10^{-4}$. In Figs 1(b) and 2(b) we display the reconstructions with 1% random noise in the data and $\alpha_\psi = \alpha_\chi = 10^{-7}$ and $\alpha_\zeta = 10^{-3}$ using Method A and Method B respectively, whereas in Fig. 1(c) we display the reconstructions with 3% random noise in the data and $\alpha_\psi = \alpha_\chi = 10^{-6}$ and $\alpha_\zeta = 10^{-1}$.

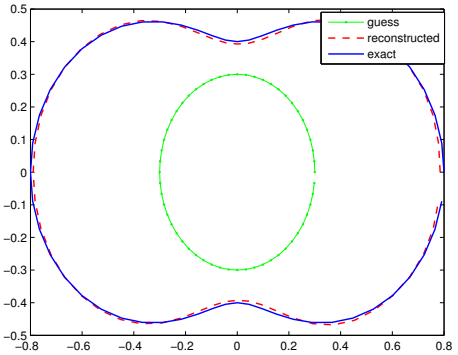

(a) ***Exact data;***

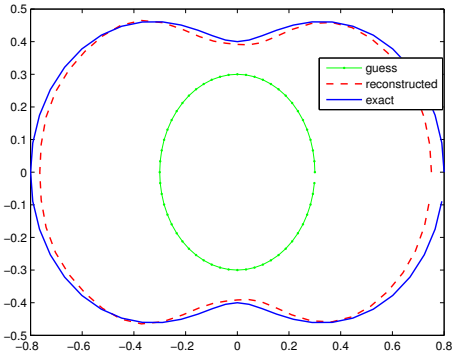

(b) 1% ***noise data.***

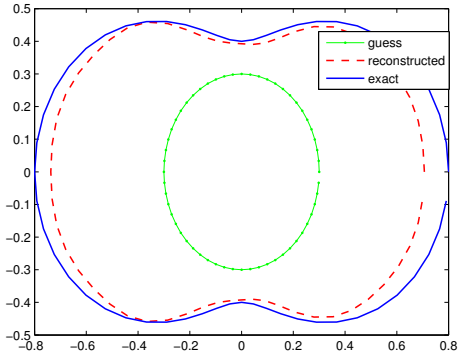

(c) 3% ***noise data.***

Figure 1: Reconstruction for ∂D_p with $k = 2$, $d = r_c(-1, 0)$ and $itera = 8$ for Method A. Here the radius of the measurement circle C is given by $r_c = 0.1$.

The second example involves the reconstruction of a peach parametrized by

$$\begin{aligned}\partial D_a =\ & (1.2 - 1/3\sin t - 1/7\sin(3t))(\cos t, \sin t) \\ :=\ & r(t)(\cos t, \sin t), \quad 0 \le t \le 2\pi\end{aligned}$$

where we choose $r_c = 0.4$, $r_o = 0.8$, $N = 60$, $m = 10$ and $k = 1$. The results are shown in Figs. 3 - 4, more specifically Figs. 3(a) and 4(a) display the reconstructions with

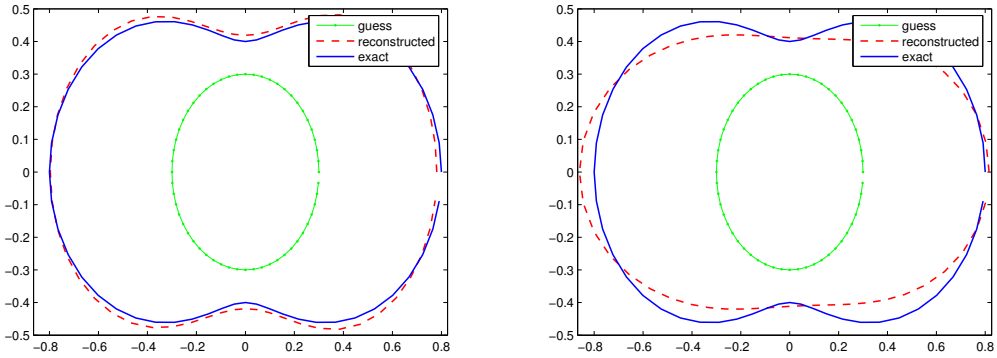

(a) ***Exact data;*** **(b)** 1% ***noise data.***

Figure 2: Reconstruction for ∂D_p with $k = 2$, $d = r_c(-1, 0)$ and $itera = 8$ for Method B. Here the radius of the measurement circle C is given by $r_c = 0.1$.

exact data and $\alpha_\psi = \alpha_\chi = 10^{-9}$ and $\alpha_\zeta = 10^{-6}$, whereas Figs. 3(b) and 4(b) with 1% random noise data and $\alpha_\psi = \alpha_\chi = 10^{-7}$ and $\alpha_\zeta = 10^{-4}$.

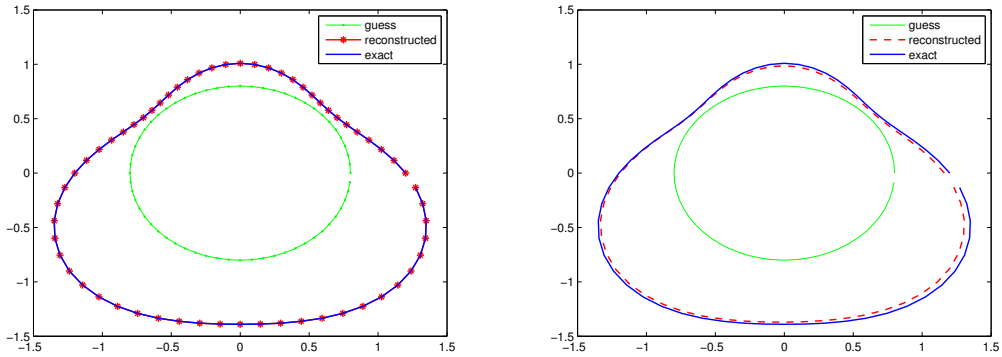

(a) ***Exact data;*** **(b)** 1% ***noise data.***

Figure 3: Reconstruction for ∂D_a with $k = 1$, $d = r_c(-1, 0)$ and $itera = 12$ for Method A. Here the radius of the measurement circle C is given by $r_c = 0.4$.

The third example considered here is a pear parametrized by

$$\partial D_r = (1.2 + 0.25\cos(3t))(\cos t, \sin t), \quad 0 \le t \le 2\pi. \tag{27}$$

The numerical results are shown in Figs. 5 - 6 where the choice of the involved parameters is $r_c = 0.48$, $r_o = 0.6$, $m = 10$, $N = 64$. In the example displayed in Figs. 5 and 6(a)-6(b), we choose $k = 1.25$ whereas in Figs. 6(c)-6(d) we choose $k = 2.25$. The reconstructions in Figs. 5(a) and 6(a) are done with exact data $\alpha_\psi = \alpha_\chi = 10^{-8}$ and $\alpha_\zeta = 10^{-2}$, and the reconstructions in Figs. 5(b) and 6(b) with 3% random noise data and $\alpha_\psi = \alpha_\chi = 10^{-5}$ and $\alpha_\zeta = 10^{-1}$. Finally for the reconstructions in Fig. 6(c) we use

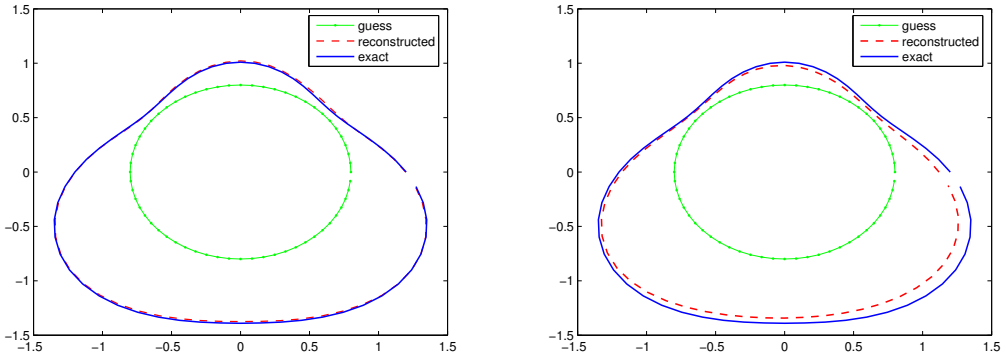

(a) ***Exact data;*** **(b)** 1% ***noise data.***

Figure 4: Reconstruction for ∂D_a with $k = 1$, $d = r_c(-1, 0)$ and $itera = 12$ for Method B. Here the radius of the measurement circle C is given by $r_c = 0.4$.

exact data with $\alpha_\psi = 3 \times 10^{-4}$ and $\alpha_\zeta = 2 \times 10^{-2}$, and in Fig. 6(d) 3% random noise data with $\alpha_\psi = 6 \times 10^{-4}$ and $\alpha_\zeta = 10^{-1}$.

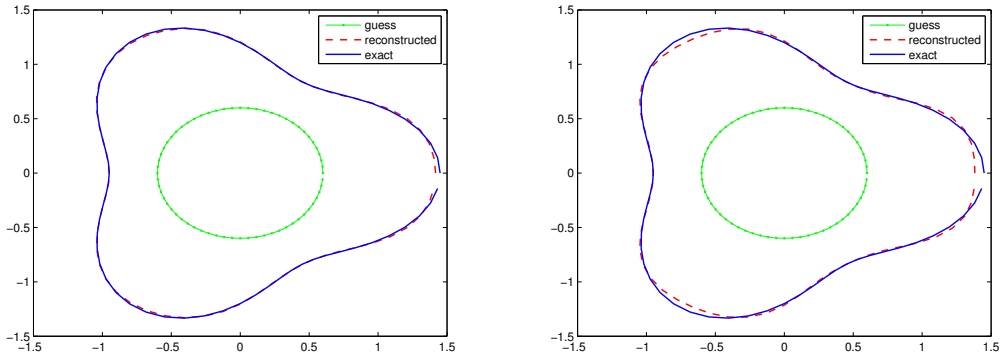

(a) ***Exact data with*** $k = 1.25$***;*** **(b)** 3% ***noise data with*** $k = 1.25$***;***

Figure 5: Reconstruction for ∂D_r with $d = r_c(-1, 0)$ and $itera = 7$ for method A. Here the radius of the measurement circle C is given by $r_c = 0.48$.

The next example involves the reconstruction of a kite parametrized by

$$\partial D_k = (0.6\cos t + 0.3\cos(2t), 0.6\sin 2t), \quad 0 \le t \le 2\pi \tag{28}$$

where we choose $r_c = 0.1$, $r_o = 0.4$, $N = 64$, $m = 8$ and $k = 2.05$. The results are shown in Fig. 7, more specifically Fig. 7(a) displays the reconstruction with exact data and $\alpha_\psi = 10^{-7}$ and $\alpha_\zeta = 3 \times 10^{-1}$, whereas Fig. 7(b) with 1% random noise data and $\alpha_\psi = 10^{-6}$ and $\alpha_\zeta = 1$. Note that $q(t)$ for ∂D_k can not be accurately represented as linear combination of few trigonometric basis functions as oppose to the previous examples. In this case the reconstruction is somewhat worse.

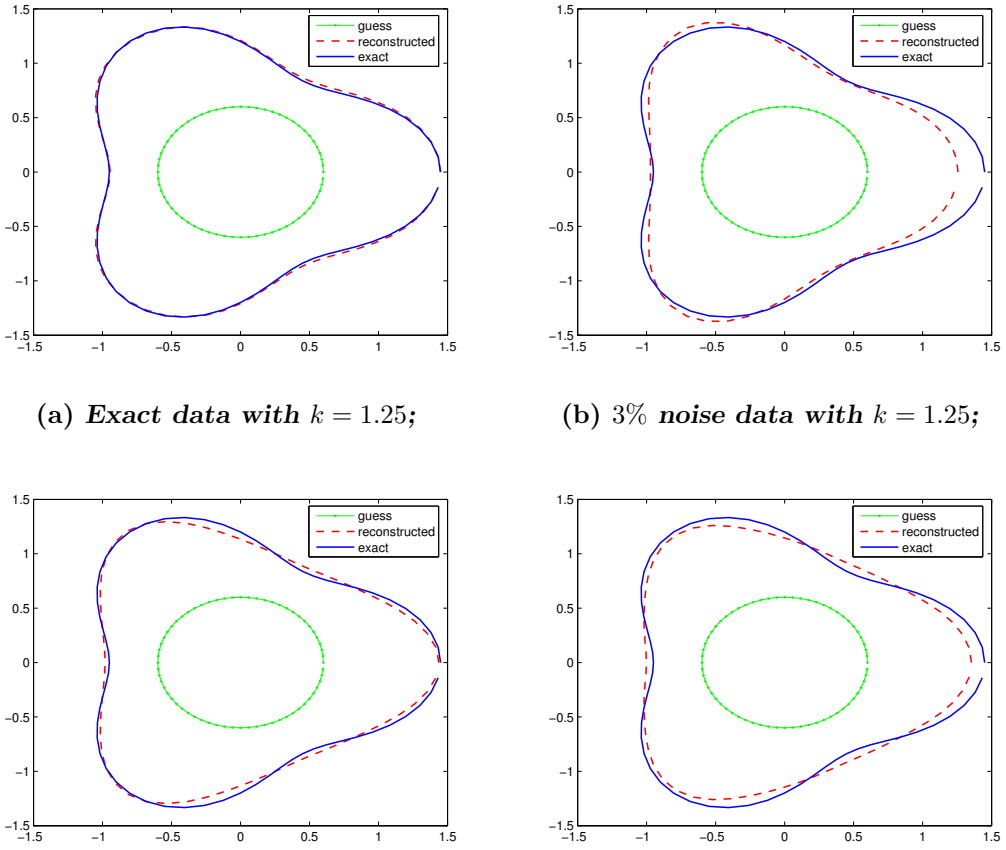

(a) ***Exact data with*** $k = 1.25$***;*** **(b)** 3% ***noise data with*** $k = 1.25$***;***

(c) ***Exact data with*** $k = 2.25$***;*** **(d)** 3% ***noise data with*** $k = 2.25$***;***

Figure 6: Reconstruction for ∂D_r with $d = r_c(-1, 0)$ and $itera = 7$ for method B. Here the radius of the measurement circle C is given by $r_c = 0.48$.

Although the interior scattering problem (1)-(2) is not properly formulated if k^2 is a Dirichlet eigenvalue of the negative Laplacian we tested the Method B for the case of a circle and k^2 close to an eigenvalue. In particular we consider the circle parametrized by

$$\partial D_c = 2\,(\cos t, \sin t)\,, \quad 0 \le t \le 2\pi. \tag{29}$$

We use $N = 60$, $k = 1.91585$, $r_c = 0.5$ and choose two different curves as initial guess, namely

$$\partial D_{ell} = \{x(t) | x(t) = (\cos t, 0.5 \sin t)\}, \quad 0 \le t \le 2\pi \tag{30}$$

where the involved parameters are $m = 10$, $\alpha_\psi = 10^{-5}$, $\alpha_\zeta = 10^{-1}$, $itera = 8$, and

$$\partial D_{cir} = \{x(t) | x(t) = (1.2 \cos t - 0.12, 1.2 \sin t + 0.1)\}, \quad 0 \le t \le 2\pi \tag{31}$$

where the involved parameters are $m = 8$, $\alpha_\psi = 10^{-5}$, $\alpha_\zeta = 10^{-3}$ and $itera = 8$.

The results and the chosen regularization parameters are shown in Fig. 8

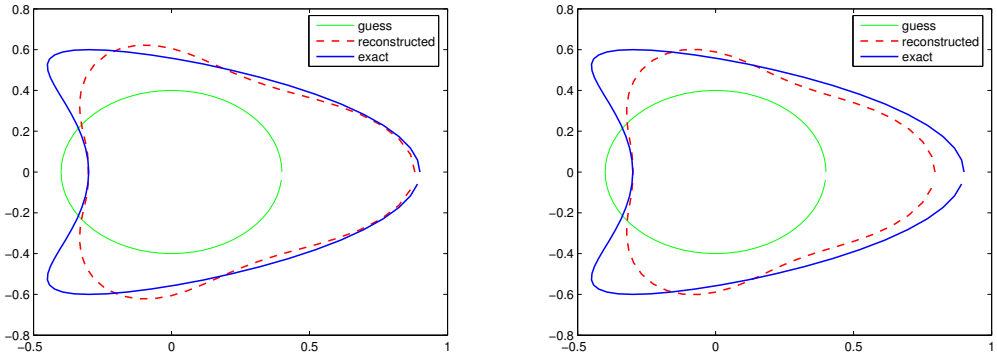

(a) *Exact data;* **(b) 1% *noise data;***

Figure 7: Reconstruction for ∂D_k with $k = 2.05$, $d = r_c(-1, 0)$ and $itera = 18$ for Method B. Here the radius of the measurement circle C is given by $r_c = 0.1$.

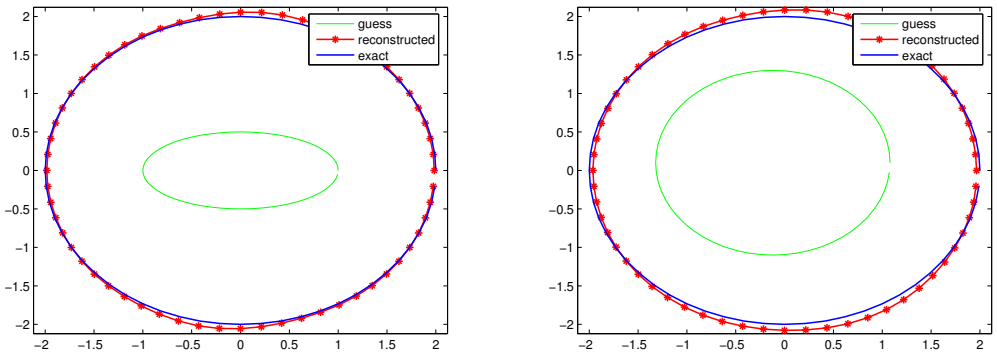

(a) *with the initial guess* ∂D_{ell}*;* **(b) *with the initial guess* ∂D_{cir}*;***

Figure 8: Reconstruction for ∂D_c with $k = 1.91585$ (which is close to a Dirichlet eigenvalue for $-\Delta$ inside ∂D_c), $d = r_c(-1, 0)$ and 1% noise in the data using Method B. Here the radius of the measurement circle C is given by $r_c = 0.5$.

Since our stopping criterion was chosen in ad-hoc manner, we present a sensitivity analysis of the reconstruction with respect to the number of iterations. To this end, we introduce the relative ℓ^2 error between the computed polar radius $r_{com}(t)$ for the boundary and the exact $r(t)$ given by

$$Error := \frac{\left(\sum_{i=1}^{2n+1} |r_{com}(t_i) - r(t_i)|^2\right)^{\frac{1}{2}}}{\left(\sum_{i=1}^{2n+1} |r(t_i)|^2\right)^{\frac{1}{2}}},$$

where $t_i = \frac{\pi}{n}(i-1)$, $i = 1, \cdots, 2n+1$. In Fig. 9 we present a plot of the ℓ^2 - error against the number of iterations for ∂D_a with 1% random noise data, $n = 30$.

The presented examples show that the proposed iterative numerical approaches work well, although Method A appears to perform somehow better than Method B. Of course, the results deteriorate as the noise level increases. We also observe that as the wave number increases the reconstruction worsen. Note that for all examples the size of the scatterer and the wave number are such that kR is small enough so that uniqueness with one source holds true, see Corollary 2.2 and Remark 2.3. Finally, our last example indicates that the proposed Newton iterative approachs (at least Method B) works well if k^2 is close to a Dirichlet eigenvalue for the cavity, despite the fact that the scattering problem is not properly formulated and the method is not theoretically justified (we use synthetic data computed based on a double-layer potential approach as for the other examples).

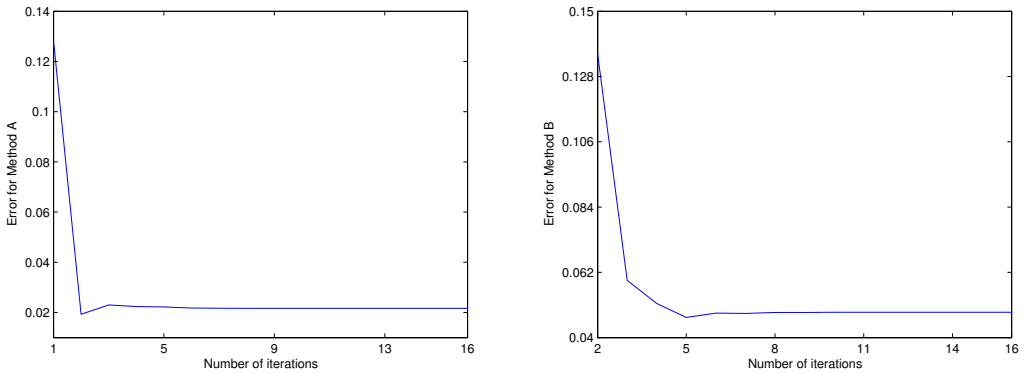

(a) *Method A;* **(b) *Method B;***

Figure 9: Relative error for ∂D_a with $k = 1$, $d = r_c(-1, 0)$ and the radius $r_c = 0.4$ of the measurement circle C.

References

[1] Angell T S and Kirsch A 2004 Optimization methods in electromagnetic radiation (New York: Springer)

[2] Cakoni F and Colton D 2006 Qualitative methods in inverse scattering theory (Berlin: Springer)

[3] Cakoni F and Kress R 2007 Integral equations for inverse problems in corrosion detection from partial Cauchy data *Inverse Probl. Imaging* 1 229–245

[4] Cakoni F, Kress R and Schuft C 2010 Integral equations for shape and impedance reconstruction in corrosion detection *Inverse Problems* 26 095012

[5] Colton D and Kirsch A 1996 A simple method for solving inverse scattering problems in the resonance region *Inverse Problems* 12 383–393

[6] Colton D and Kress R 1998 Inverse acoustic and electromagnetic scattering theory (Berlin: Springer)

[7] Colton D, Piana M and Potthast R 1997 A simple method using Morozov's discrepancy principle for solving inverse scattering problems *Inverse Problems* 13 1477–1493

[8] Colton D and Sleeman B D 1983 Uniqueness theorems for the inverse problem of acoustic scattering *IMA J. Appl. Math.* 31 253–259

[9] Gintides D 2005 Local uniqueness for the inverse scattering problem in acoustics via the Faber-Krahn inequality *Inverse Problems* 21 1195–1205

[10] Ivanyshyn O, Kress R and Serranho P 2010 Huygens' principle and iterative methods in inverse obstacle scattering *Adv. Comput. Math.* 33 413–429

[11] Ivanyshyn O and Johansson T 2007 Nonlinear integral equation methods for the reconstruction of an acoustically sound-soft obstacle *J. Integral Equations Appl.* 19 289–308

[12] Ivanyshyn O and Kress R 2006 *Nonlinear integral equations in inverse obstacle scattering (Mathematical methods in scattering theory and biomedical engineering)* eds Fotiadis D I and Christos V M (New Jersey: World Sci. Publ.) pp 39–50

[13] Ivanyshyn O and Kress R 2008 Inverse scattering for planar cracks via nonlinear integral equations *Math. Methods Appl. Sci.* 31 1221–1232

[14] Jakubik P and Potthast R 2008 Testing the integrity of some cavity—the Cauchy problem and the range test *Appl. Numer. Math.* 58 899–914

[15] Johansson T and Sleeman B D 2007 Reconstruction of an acoustically sound-soft obstacle from one incident field and the far-field pattern *IMA J. Appl. Math.* 72 96–112

[16] Kress R and Rundell W 2005 Nonlinear integral equations and the iterative solution for an inverse boundary value problem *Inverse Problems* 21 1207–1223

[17] Lee K -M 2006 Inverse scattering via nonlinear integral equations for a Neumann crack *Inverse Problems* 22 1989–2000

[18] McLean, W., 2000 *Strongly Elliptic Systems and Boundary Integral Equations* Cambridge University Press.

[19] Potthast R 1994 Fréchet differentiability of boundary integral operators in inverse acoustic scattering *Inverse Problems* 10 431–447

[20] Qin H -H and Colton D 2010 The inverse scattering problem for cavities *Applied Num. Math.* (to appear).

[21] Qin H -H and Colton D 2010 The inverse scattering problem for cavities with impedance boundary condition *Advances Comp. Math.* (to appear).